Numerical Simulation of a Tubular Polymerization Reactor

D. LYNCH and C. KIPARISSIDES, *Department of Chemical Engineering, The University of Alberta, Edmonton, Alberta, Canada*

Synopsis

A mathematical model for a tubular emulsion polymerization reactor is developed. The partial differential equations describing the mass balances on initiator, monomer, and number of polymer particles are numerically solved using an implicit–explicit scheme based on the Crank–Nicholson method. The model adequately simulates experimental results reported by Rollin and co-workers and sufficiently explains the unusual behavior of the reactor when operating at relatively low emulsifier concentrations.

INTRODUCTION

In heterophase polymerizations such as suspension and emulsion polymerization, where the viscosity is relatively independent of monomer conversion and fluid mechanical factors associated with heat transfer and pumping can be readily overcome, the use of tubular reactors in the commercial production of polymers has important advantages. Tubular continuous reactors can be used to increase the heat transfer area and thus improve temperature control[1] and generally give lower operating cost and more uniform product stream. In addition, utilization of continuous tubular reactors can increase safety for production people due to minimal exposure to and handling of chemical products.

The two most significant studies performed in this area have been by Ghosh and Forsyth[2] and Rollin et al.[3,4] Ghosh and Forsyth performed an experimental and theoretical study of the emulsion polymerization of styrene in a tubular reactor for Reynolds numbers up to 210 and very high soap concentrations. Under these conditions they were able to obtain operation of the reactor without plugging and conversions as high as 90%. In their attempt to model the tubular reactor, however, they assumed that the number of polymer particles remained constant during the polymerization. Then, a fit between the experimental and predicted conversions was obtained by empirically evaluating the number of polymer particles through the use of their experimental data.

The work of Rollin et al.[3,4] is particularly interesting as some unusual results are presented. They experimentally found that the emulsion Reynolds number had a large effect on the conversion of styrene in a tubular emulsion polymerization reactor. For a particular reaction mixture, they found that conversions of 100% were approached in a batch reactor, while limiting conversions less than 100% were reached when a tubular reactor was used. Also, they observed that, when operating in the turbulent flow region, the final conversion decreased as the Reynolds number was increased. Rollin et al. explained this behavior via various qualitative arguments, as they did not develop any models for their system.

It was felt that the arguments presented by Rollin et al. were not sufficient for describing the observed behavior. Hence, it was decided to attempt to predict their experimentally obtained results by developing a mathematical model of the system.

MODEL DEVELOPMENT

Rollin et al.[3] used a closed-loop tubular reactor to carry out the emulsion polymerization of styrene. The reactor system consisted of a 7.7-mm-inside-diameter stainless tube 18.9 m long which was jacketed by a 20.0-mm copper tubing. Emulsification was achieved by circulating the ingredients (monomer, water, and emulsifier) inside the reactor for $\frac{1}{2}$ hr by a Moyno pump at a constant flow rate. The flow rate was then adjusted to the desired value and the initiator metered in during a period equal to the residence time for the chosen flow rate.

To model the emulsion polymerization of styrene in a tubular reactor, the following assumptions were made in writing the mass balances for the initiator, monomer, and number of polymer particles: (1) the emulsion is undergoing plug flow with a constant axial velocity; (2) the reactor operates at a constant temperature; (3) the diffusion coefficients of the initiator in the emulsion is constant; (4) there is negligible axial diffusion of monomer and polymer particles in the emulsion; (5) Smith–Ewart case 2 kinetics apply at all conversions, that is, the number of radicals per polymer particle is constant at 0.5.

Utilizing the above assumptions, the mass balances on initiator, monomer, and number of particles in terms of dimensionless time and distance become

$$\frac{\partial I}{\partial T} = -\frac{\partial I}{\partial Z} + \left(\frac{D}{uL}\right)\frac{\partial^2 I}{\partial Z^2} + R_d\left(\frac{L}{u}\right) + F\left(\frac{L}{u}\right) \tag{1}$$

$$\frac{\partial M}{\partial T} = -\frac{\partial M}{\partial Z} + R_p\left(\frac{L}{u}\right) \tag{2}$$

$$\frac{\partial N}{\partial T} = -\frac{\partial N}{\partial Z} + (R_i - R_c - R_f)\left(\frac{L}{u}\right)N_a \tag{3}$$

where the various symbols are defined in the nomenclature section. It is more convenient to write eq. (2) in terms of conversion; hence, let

$$M = M_0(1 - X) \tag{4}$$

then eq. (2) becomes

$$\frac{\partial X}{\partial T} = -\frac{\partial X}{\partial Z} - R_p\left(\frac{L}{uM_0}\right) \tag{5}$$

The rate expressions in the above equations are given by

$$R_d = -k_d I \tag{6}$$

$$R_p = -k_p[M_p]N_p/2N_a \tag{7}$$

$$R_i = 2fk_d I \tag{8}$$

$$R_c = R_i A_p/a_s[S] \tag{9}$$

$$R_f = KN_p^2 \tag{10}$$

$$K = f(\text{Reynolds number}) \tag{11}$$

$$F = F(T,Z) \tag{12}$$

where R_d is the rate of initiator decomposition and R_p is the polymerization rate; R_i denotes the rate of initiation of radicals, R_c the rate of radical capture into polymer particles, and R_f is the rate of particle coalescence. In eq. (9), it is assumed that radical capture occurs according to the collision theory, that is, R_c will be proportional to the total surface area of polymer particles, A_p. Therefore, as the number of polymer particles increases, the capture rate R_c grows and approaches the initiation rate. Adamson[5] gives the rate of particle coalescence, R_f, between equal sized particles to be equal to N_p^2 times the rate constant of coalescence, K, eq. (10). K is a complex function of temperature, initiator, and emulsifier concentrations, viscosity and dielectric constant of the medium, electrostatic potential energy for repulsion and attraction, as well as of agitation speed.

The degree of agitation or otherwise the intensity of the shear field influences the rate of particle coalescence, as can be seen in the work of Nomura et al.[6] and Kiparissides et al.[7] In eq. (11), we have assumed that K is a function of Reynolds number, which is true if all other variables affecting K are practically constant. Rollin et al.[3] actually carried out their experiments in a tubular reactor by varying only the emulsion Reynolds number and keeping all the other variables, the polymerization temperature, initiator, emulsifier, and monomer concentrations, constant. Particle coalescence should be important in systems with high initiation rates and where stabilization of particles by surfactants is not completely effective. In such cases, there can be an overshoot in N_p early in the polymerization. However, as the particle number reaches some very high value, the rate of coalescence exceeds the rate of particle generation $(R_i - R_c)$ and the number of particles begins to decrease.

In eq. (7), $[M_p]$ is the monomer concentration in the polymer phase given as

$$[M_p] = \frac{(1 - X_c)d_m}{(1 - X_c + X_c d_m/d_p)\tilde{M}} \qquad 0 \le X \le 0.27 \tag{13}$$

$$[M_p] = \frac{(1 - X)d_m}{(1 - X + X d_m/d_p)\tilde{M}} \qquad X > 0.27 \tag{14}$$

The term F for the rate of addition of initiator requires more attention owing to the way in which the initiator was added to the reactor. In the experimental runs of Rollin et al.,[3] the initiator was added to the reactor over a time period equal to one residence time of the reactor, such that the total amount of initiator added would be sufficient to create an overall composition of 2.55 g mole/m^3 in the reactor. If all of the initiator is added to the reactor element of volume δ, then F can be defined by

$$F = 0.0 \qquad T > 0, \quad Z > \delta \tag{15}$$

$$F = 0.0 \qquad T \ge 1, \quad Z = Z \tag{16}$$

$$F = \frac{2.55u V}{L\delta} \qquad 0 \le T < 1, \quad 0 \le Z \le \delta \tag{17}$$

The evaluation of A_p, total surface area of polymer particles, in eq. (9) presents some problem, as strictly speaking A_p is given by

$$A_p = [(4\pi)^{1/2}3\mu L/u]^{2/3} \int_0^T (T - T_0)^{2/3}(\partial N_p/\partial T_0)_{T_0} \, dT_0 \qquad (18)$$

The evaluation of the above integral is extremely cumbersome; hence, the simplification of assuming a uniform polymer particle size will be used. This assumption results in the following set of equations for determining A_p:

$$A_p = (36\pi)^{1/3}N_p^{1/3}V_T^{2/3} \qquad (19)$$

$$V_T = \frac{V_p}{1 - \phi} \qquad (20)$$

$$V_p = \frac{M_0\tilde{M}X}{d_p} \qquad (21)$$

$$\phi = \frac{1 - X}{1 - X(1 - d_m/d_p)} \qquad X > 0.27 \qquad (22)$$

$$\phi = \frac{1 - X_c}{1 - X_c(1 - d_m/d_p)} \qquad 0 < X \le 0.27 \qquad (23)$$

The initial conditions to be used in the solution of the above equations are

$$I(0,Z) = 0 \qquad (24)$$

$$X(0,Z) = 0 \qquad (25)$$

$$N_p(0,Z) = 0 \qquad (26)$$

where $X = X(T,Z)$, $N_p = N_p(T,Z)$, and $I = I(T,Z)$. The fact that the reactor is actually a continuous loop with a pump circulating the emulsion results in the feed to the reactor being defined by

$$I(\text{feed}) = I(T,1) \qquad (27)$$

$$X(\text{feed}) = X(T,1) \qquad (28)$$

$$N_p(\text{feed}) = N_p(T,1) \qquad (29)$$

The solution of the preceding equations was attempted by utilizing a finite difference scheme. For the purposes of applying the finite difference method for solving eqs. (1)–(3), the reactor was divided into M nodes ($M - 1$ elements) (Fig. 1). Difference equations were written around each of the M nodes, resulting in $3M$ simultaneous equations to be solved at each time step. An implicit–explicit scheme based on the Crank–Nicholson method was used, where, for stability considerations, a backward difference approximation for the first derivative terms are necessary. The details of the actual difference equations used are given in Appendix B.

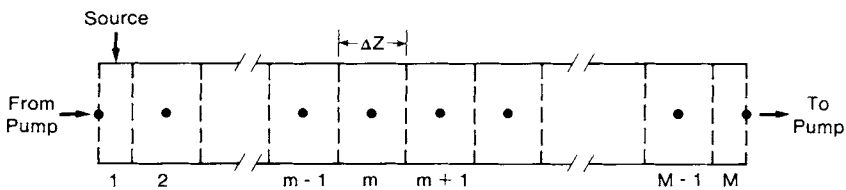The complexity of the problem is reduced somewhat by the fact that the so-

Fig. 1. Reactor approximation into $M - 1$ elements.

lution for the initiator concentration is not coupled to the solutions for the conversion or the number of polymer particles. The steps followed in obtaining the solution at each time increment were as follows:

(1) Determine the initiator distribution explicitly via a modified Thomas algorithm.

(2) Simultaneously determine the conversion and the number of particles distributions explicitly (modified Thomas algorithm) using the previous values of X and N_p as initial guesses in the reaction rate calculations (R_p, R_c, and R_f).

(3) Iterate on the calculated values of X and N_p until convergence is obtained using the most recent values of X and N_p in the reaction rate calculations.

(4) If the final time has not been reached, then increment the time and return to step 1.

The above steps were implemented in a Fortran computer program designed to run on a HP1000 21MXE minicomputer. The algorithm was found to be unconditionally stable for all values of ΔT and ΔZ; however, for a particular choice of ΔZ, it was only convergent for values of $\Delta Z/\Delta T \geq 1$. An asymptotic convergence of the solution to its final value was obtained for values of ΔZ smaller than 0.01. The small values of ΔZ are necessitated by the fact that setting ΔZ = 0.005 is equivalent to dividing the actual reactor into elements which are 0.1 m long. From a purely physical point of view, this reactor division is still quite coarse. Intuitively, the division of the reactor into M discrete elements is equivalent to assuming that the plug-flow reactor is actually M CSTRs in series. In the limit of M going to infinity this approximation will be valid, but for finite values of M some error will always be encountered.

DISCUSSION

Once the stability and convergence of the algorithm were established, several runs were made to match the average conversion from the model output with the reported experimental conversions of Rollin et al.[3] In all simulations, the step sizes used were ΔZ = 0.01 and ΔT = 0.01. The values of the different parameters appearing in eqs. (1)–(23) are listed in Appendix A. The same values of the parameters were used for all the simulated runs.

The main problem encountered in attempting to match the model with the experimental results[3] was that several of the experimental runs indicate the occurrence of an induction period which cannot be simulated by this model in its present form. One method of simulating an induction period would be to make the initiator efficiency a function of time, i.e., $f = f_0[1 - \exp(-T)]$. However, this was not included in the model.

The overall results for all the simulated cases are given in Figure 2. It is clear that the predicted values are in very good agreement with the experimental results. For each simulated run a different value of the adjustable parameters K in the expression for the rate of coalescence eq. (11) was used. By plotting the values of K versus Reynolds number in a log–log scale, we were able to derive the following relationship for the rate constant for particle coalescence:

$$K = C \text{ (Reynolds number)}^\alpha \tag{30}$$

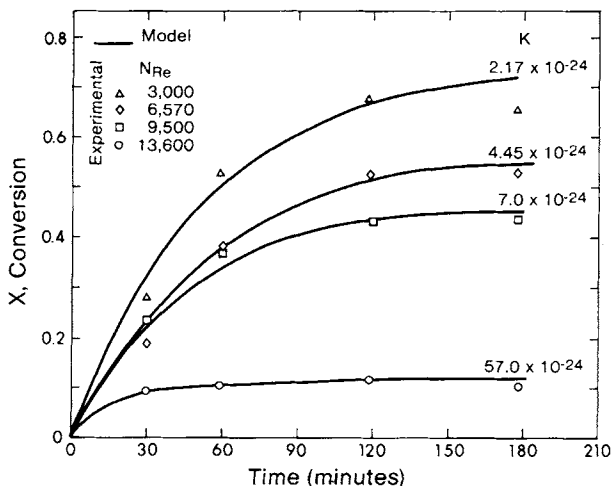where C is a constant and the parameter α is approximately equal to 1. Equation

Fig. 2. Overall comparison between model and experimental results ($T = 60°C$, $M_0 = 1731$ g mole/m^3 emulsion, $S = 5.34$ g mole/m^3 emulsion, $I = 2.55$ g mole/m^3 emulsion).

(30) indicates that the rate constant for particle coalescence will increase as the Reynolds number increases in the turbulent flow region. A higher coalescence rate would cause an actual reduction of the number of polymer particles thus resulting in a decrease of the polymerization rate, eq. (7). A similar behavior has been reported for continuous stirred tank and batch latex reactors[6,7] where it was shown that an intense shear field at higher agitation speeds could cause excessive particle agglomeration. This appears conceivable since particle coalescence by rigorous stirring might be accompanied by turbulent flow. The local excess kinetic energy imparted upon particles in a turbulent flow region and the simultaneous and temporary strong deformation of the electrostatic double layer of the polymer particles due to an intense shear field could lead to a mutual approach of particles and finally to aggregation.

The effect of the coalescence rate constant on conversion at a Reynolds number of 4330 is shown in Figure 3. It can be seen that conversion decreases as the rate constant K increases.

The time variation of the average number of particles in the reactor for the first 10 min of simulation with a Reynolds number of 4330 is given in Figure 4, and the variation of N_p with time for all the simulated runs up to a time of 2 hr is given in Figure 5. From Figures 4 and 5, it is seen that the total number of particles in the reactor increases rapidly, reaching its maximum value ($\sim 2 \times 10^{17}$ particles/l.) in about 5 min at a conversion value of approximately 5%. This model behavior with regards to N_p is very similar to the actual physical behavior of operating batch reactors. A comparison between model and experimental conversion values for a batch reactor is presented in Figure 6. For this case, it is assumed that the rate of particle coalescence is negligible. It can be seen that there is a good agreement between experimental and predicted results. It is interesting to note that conversion values up to 100% are obtained after 3 hr of reaction time. On the contrary, limiting conversions less than 100% (Fig. 2) due mainly to particle agglomeration are observed for the tubular reactor when operating under similar conditions.

The effects of agitation (shear field) and the presence of oxygen or other im-
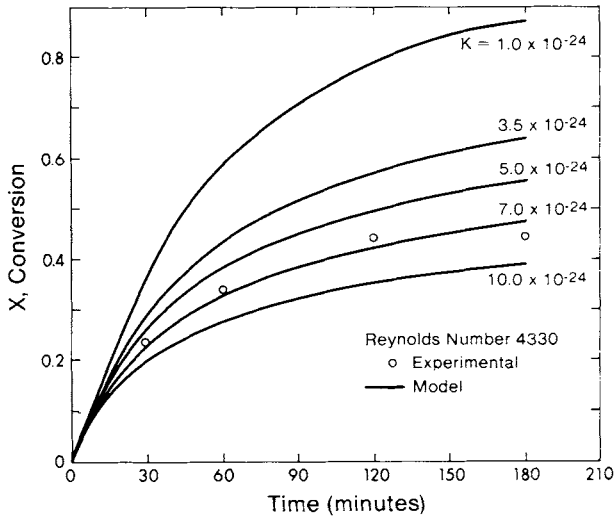
Fig. 3. Effect of the coalescence rate constant (K) on the limiting conversion value (N_{Re} = 4330).

purities on the rate of polymerization in a latex reactor have been experimentally studied by Nomura et al.[6] and Kiparissides et al.[7] The results of their independent studies are summarized as follows: (1) A strong shear field can deform the electrostatic double layer of the particles thus increasing the mechanical
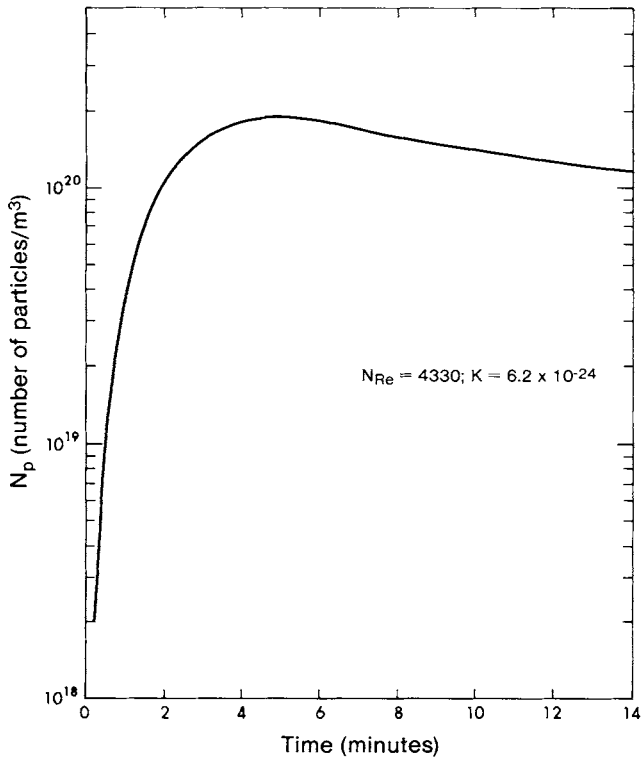

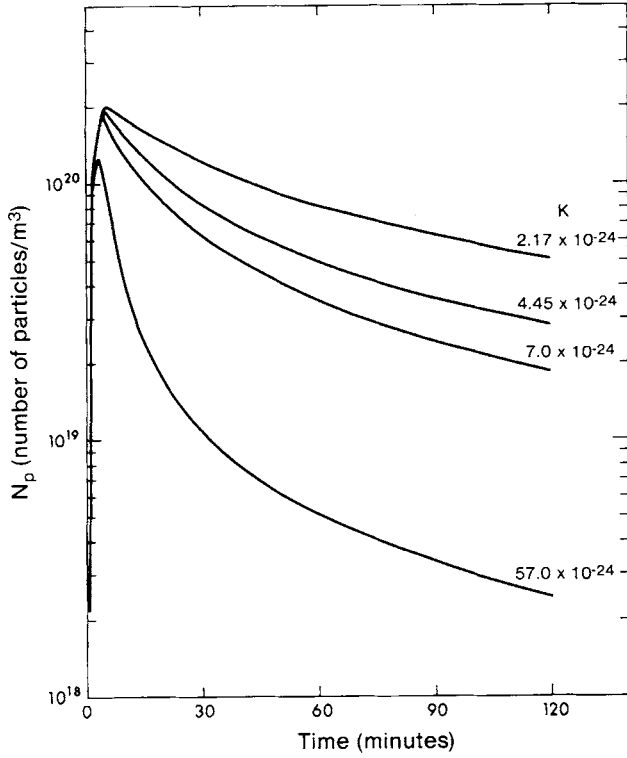Fig. 4. Number of polymer particles vs. time.

Fig. 5. Number of polymer particles at different Reynolds numbers vs. time.

coagulation. (2) Stirring can reduce the number of micelles thus reducing the number of polymer particles. (3) Stirring can significantly affect the course of polymerization in the presence of oxygen traces or other dissolved impurities.
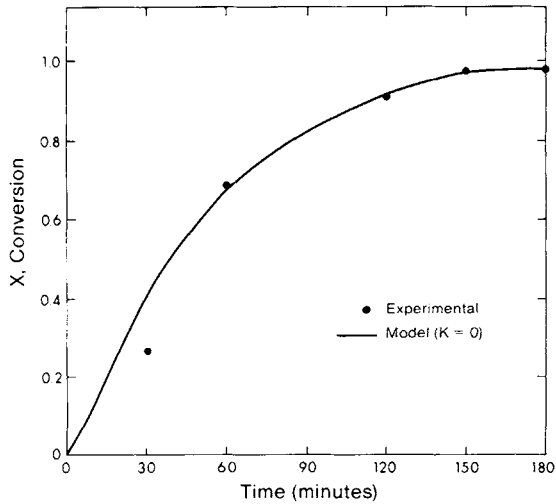
Fig. 6. Comparison between model ($K = 0$) and batch reactor experimental results ($T = 60°C$, $M_0 = 1731$ g mole/m^3 emulsion, $S = 5.34$ g mole/m^3 emulsion, $I = 2.55$ g mole/m^3 emulsion).

Kiparissides et al.[7] examined the stability and fouling of a latex in relation to DLVO theory. They showed that the electrolyte concentration, the surface charge density of a particle, the reciprocal of the particle radius, and an agitation parameter could dramatically affect the stability of the latex product.

CONCLUSIONS

Experimental results reported by Rollin et al. on the continuous emulsion polymerization of styrene in a tubular reactor were successfully simulated by the proposed mathematical model. It was shown that the rate of polymerization decreases with increasing Reynolds number when the polymerization was carried out in the turbulent flow regime. An expression for the coalescence rate constant was derived as a function of the Reynolds number. It was found that at higher Reynolds numbers, under turbulent flow conditions, the rate of particle coalescence increased resulting in a lower final conversion value. The last finding is in agreement with experimental results reported in the literature for batch and continuous latex reactors. The influence of axial diffusion in eq. (1) was found to be negligible and hence could be eliminated from future models. Although we have assumed that average number of radicals per particle, $\bar{q}$, is equal to 0.5, a more general expression can be used[8] to account for values of $\bar{q}$ different from 0.5 occurring at higher conversions (>60%).

The developed model can provide reactor simulations by specifying reactor operating conditions and thus be used for feasibility studies on the commercial production of polymer and copolymer in tubular reactors.

Notation

a_s	specific surface area of emulsifier molecule, m^2/m^3
A_p	total surface area of polymer particles, m^2
C	empirically determined constant
d_m	density of monomer, kg/m^3
d_p	density of polymer, kg/m^3
D	diffusivity of initiator in water, m^2/sec
f	initiator efficiency factor
F	rate of initiator addition, g mole/m^3 sec
I	initiator concentration, g mol/m^3
k_d	initiator decomposition rate constant, sec^{-1}
k_p	propagation rate constant, m^3/g mole sec
K	adjustable parameter in the rate of particle coalescence
L	length of the reactor, m
M	overall monomer concentration in the emulsion, g mole/m^3
M_0	initial monomer concentration, g mole/m^3
M_p	monomer concentration in the polymer phase, g mole/m^3
$\bar{M}$	molecular weight of the monomer, kg/g mole
N_a	Avogadro's number
N_p	polymer particle concentration, no. of particles/m^3 emulsion
R_c	rate of radical capture by polymer particles, g mole/m^3 sec
R_d	rate of initiator decomposition, g mole/m^3 sec
R_f	rate of particle coalescence, g mole/m^3 sec
R_i	rate of initiation, g mole/m^3 sec
R_p	rate of polymerization, g mole/m^3 sec
S	effective emulsifier concentration ($S = S_i - S_{cmc}$), g mole/m^3
S_i	initial overall emulsifier concentration, g mole/m^3

S_{cmc}　emulsifier concentration necessary to achieve the critical micelle concentration, g mole/m^3
t　　time, sec
T　　dimensionless time, tu/L
T_o　dummy time variable for exact A_p calculation, eq. (18)
u　　emulsion velocity, m/sec
V　　reactor volume, m^3
V_p　specific volume of polymer particles, m^3/m^3 emulsion
V_T　specific volume of polymer particles swollen with monomer, m^3/m^3 emulsion
X　　monomer fractional conversion
X_c　conversion at which the separate monomer phase disappears
z　　reactor axial distance, m
Z　　dimensionless reactor axial distance, z/L
δ　　reactor volume element to which initiator is added, m^3
ϕ　　volume fraction of monomer in the polymer phase
μ　　growth rate of polymer particles, m^3/sec

APPENDIX A

Constants Used in Reactor Simulation

$a_s = 5.62 \times 10^5$ m^2/g mole
$d_m = 900$ kg/m^3
$d_p = 1040$ kg/m^3
$D = 3.1 \times 10^{-9}$ m^2/sec
$f = 0.9$
$k_d = 5.0 \times 10^{-7}$ sec^{-1}
$k_p = 0.385$ m^3/g mole sec
$L = 18.9$ m
$M_0 \approx 1731$ g mole/m^3 emulsion
$M = 0.104$ kg/g mole
$S = 5.34$ g mole/m^3 emulsion
$u = 0.1782; 0.2577; 0.3908; 0.5648; 0.8117$ m/sec
$V = 8.8 \times 10^{-4}$ m^3
$X_c = 0.27$

APPENDIX B

For an interior node m where $2 \leq m \leq M - 1$ (Fig. 1), the general difference equations for initiator [eq. (1)], conversion [eq. (5)], and number of polymer particles [eq. (3)] can be written

$$I_m^{p+1}\left(\frac{\Delta Z}{\Delta T} + \frac{1}{2} + \frac{D}{uL\Delta Z} + \frac{Lk_d\Delta Z}{2u}\right) - I_{m-1}^{p+1}\left(\frac{1}{2} + \frac{D}{2uL\Delta Z}\right) - I_{m+1}^{p+1}\left(\frac{D}{2uL\Delta Z}\right)$$
$$= I_m^p\left(\frac{\Delta Z}{\Delta T} - \frac{1}{2} - \frac{D}{uL\Delta Z} - \frac{Lk_d\Delta Z}{2u}\right) + I_{m-1}^p\left(\frac{1}{2} + \frac{D}{2uL\Delta Z}\right) + I_{m+1}^p\left(\frac{D}{2uL\Delta Z}\right) \quad \text{(B-1)}$$

$$X_m^{p+1}\left(\frac{2\Delta Z}{\Delta T} + 1\right) - X_{m-1}^{p+1} = X_m^p\left(\frac{2\Delta Z}{\Delta T} - 1\right) + X_{m-1}^p - R_p\left(\frac{L}{u}\right)\left(\frac{2\Delta Z}{M_0}\right) \quad \text{(B-2)}$$

$$N_m^{p+1}\left(\frac{2\Delta Z}{\Delta T} + 1\right) - N_{m-1}^{p+1} = N_m^p\left(2\frac{\Delta Z}{\Delta T} - 1\right) + N_{m-1}^p + (R_i - R_c - R_f)\left(\frac{L}{u}\right)(N_a 2\Delta Z) \quad \text{(B-3)}$$

For node 1,

$$I_1^{p+1}\left(\frac{\Delta Z}{\Delta T} + 1 + \frac{D}{uL\Delta Z} + \frac{k_dL\Delta Z}{2u}\right) - I_M^{p+1} - I_2^{p+1}\left(\frac{D}{uL\Delta Z}\right)$$
$$= I_1^p\left(\frac{\Delta Z}{\Delta T} - 1 - \frac{D}{uL\Delta Z} - \frac{k_dL\Delta Z}{2u}\right) + I_M^p + I_2^p\left(\frac{D}{uL\Delta Z}\right) \quad \text{(B-4)}$$

$$X_1^{p+1}\left(\frac{\Delta Z}{\Delta T} + 1\right) - X_M^{p+1} = X_1^p\left(\frac{\Delta Z}{\Delta T} - 1\right) + X_M^p - R_p\left(\frac{L}{u}\right)\left(\frac{\Delta Z}{M_0}\right) \quad \text{(B-5)}$$

$$N_1^{p+1}\left(\frac{\Delta Z}{\Delta T} + 1\right) - N_M^{p+1} = N_1^p\left(\frac{\Delta Z}{\Delta T} - 1\right) + N_M^p + (R_i - R_c - R_f)\left(\frac{L}{u}N_a\Delta Z\right) \quad \text{(B-6)}$$

Similar difference equations to eqs. (B-4)–(B-6) are written for node M. Superscript p stands for time increments and subscript m for space division.

References

1. T. Smith, Paper presented at the Emulsion Polymer Symposium held at Lehigh University, March 1975.

2. M. Ghosh and T. H. Forsyth, *Continuous Emulsion Polymerization of Styrene in a Tubular Reactor*, ACS Symp. Ser. No. 24, 1976, p. 367.

3. A. L. Rollin, I. Patterson, R. Huneault, and P. Bataille, *Can. J. Chem. Eng.*, **55,** 565 (1977).

4. A. L. Rollin, I. Patterson, J. Archambault, and P. Bataille, in *Polymerization Reactors and Processes Symposium*, J. N. Henderson and T. C. Button, Eds., ACS Symp. Ser. No. 104, 1979, p. 113.

5. A. W. Adamson, *Physical Chemistry of Surfaces*, 2nd ed., Wiley-Interscience, New York, 1967.

6. M. Nomura, M. Harada, W. Eguchi, and S. Nagata, *J. Appl. Polym. Sci.*, **16,** 835 (1972).

7. C. Kiparissides, J. MacGregor, and A. Hamielec, *Can. J. Chem. Eng.*, **58,** 48 (1980).

8. K. W. Min and W. H. Ray, *J. Macromol. Sci., Rev. Macromol. Chem.*, **C11,** 177 (1974).